measured in units of the diffraction length $(\lambda r/2)^{\frac{1}{2}}$. Inside the shadow region the polarization contribution is negative. Outside the shadow region, there are two terms to the polarization, one of which oscillates with zero integral, and the other of which is positive and shown by the dashed line of Fig. 3.

The arrows drawn in Fig. 2 show the direction of the electric vector present in excess in the diffraction region. The observer at O will see a net negative polarization, for, compared to the observer N, he sees an additional shadow area polarized parallel to the plane of incidence and has his view of an area of positive polarization obscured by the object.

A piece of opaque lunar dust does not precisely duplicate the diffraction conditions represented by an infinitely conductive, infinitesimally thick, half plane. It does, however, preserve the physical characteristics which cause the polarization; namely, a diffracting edge which screens the electric field by induced currents. There is a difference between driving screening currents parallel and perpendicular to the diffracting edge, because of the surface charge generated by a normal component of the current. It is this difference which distinguishes the two polarizations. The polarization of light in the shadow region for diffraction of visible light by a steel knife edge was measured by Jentzsch (*7*). Under these less ideal circumstances of both the dielectric properties and geometry, the measured polarization in the shadow region was about twice as large as that of the idealized theory, and of the same sign. As expected, the basic electromagnetic effect of polarization by diffraction around an opaque dielectric obstacle seems a qualitative effect, existing under circumstances far from those ideal cases readily calculated.

Consider a model of a lunar surface consisting of opaque "particles" of low albedo (so that multiple reflections can be ignored—a good approximation for an albedo of the order of 0.1, like that of the moon). Each particle, if particles are loosely packed, produces a "shadow" on the other particles which can collectively be regarded as a diffusing screen. With such a model, a lunar polarization of

$$P = \frac{I_{\perp} - I_{\parallel}}{I_{\perp} + I_{\parallel}} \approx -\frac{\lambda}{d}\,\frac{f}{\pi}\left[\ln\left(1 + \frac{\pi}{2}\,\frac{d^2}{\lambda r}\right)\right] \qquad (2)$$

is obtained as the saturation polarization to be expected for angles larger than the diffraction angle $(\lambda/2r)^{\frac{1}{2}}$. The dependence d^{-1} on the length d of the side of the square originates in the ratio of edge length (which produces polarized return) to the total return (proportional to the area of the square). The factor f is a depolarization factor which represents the fact that half the source of the lunar polarization is light diffracted before striking the diffusing screen. This light will be partially depolarized on reflection. Dollfus (*1*) has measured this depolarization factor to be 1/3, so a value of 2/3 for f is appropriate. The maximum negative lunar polarization of -0.012 can be produced by Eq. 2 for a wavelength of 5000 Å, a particle size of 5 microns, and a particle separation of the order of magnitude of the particle size.

While there are no direct experiments which show this polarization mechanism to be that responsible for the negative lunar polarization, two qualitative results from laboratory experiments on simulated lunar surfaces are in striking agreement with the theory. First, the negative polarization at small angles seems to be a general characteristic of reflection from powders having irregular opaque grains of sufficiently small size, relatively independent of the details of particle shape and composition (*1–3*). Second, Dollfus (*8*) has found that dark powders which produce a negative polarization at small angles do not produce this negative polarization when well-separated free-falling grains are examined. In this experiment the effect of shadow would be absent.

It is tempting to infer, from laboratory simulation, a particle size from polarization measurements. Particle size cannot be precisely defined for an unknown structural form. If the present mechanism is correct, however, there must be of the order of 10^6 cm of *shadow-producing* edges per square centimeter to explain the lunar polarization. Such a surface has at least one typical dimension of its subunits of the order of 10 microns.

J. J. Hopfield

Department of Physics, Princeton University, Princeton, New Jersey

References and Notes

1. A. Dollfus, in *Physics and Astronomy of the Moon*, Z. Kopal, Ed. (Academic Press, New York, 1962), p. 131 ff.
2. R. B. Baldwin, *The Measure of the Moon* (Univ. of Chicago Press, Chicago, 1963), pp. 248–267.
3. B. Hapke, *Ann. N.Y. Acad. Sci.* **123**, 711 (1965).
4. See, for example, Baldwin, *2*, pp. 254–255, and the theoretical study by B. Hapke, *J. Geophys. Res.* **C8**, 4571 (1963).
5. J. van Diggelen, *Planetary Space Sci.* **13**, 271 (1965).
6. M. Born and E. Wolf, *Principles of Optics* (Pergamon Press, New York, 1959), pp. 552ff.
7. F. Jentzsch, *Ann. Physik* **84**, 292 (1927–28).
8. A. Dollfus, *Ann. Astrophys.* **19**, 71 (1956).
9. B. Lyot, *Ann. Obs. Paris* **8**, Fasc. 1 (1929).
10. This investigation was carried out at a meeting of the "Tycho" study group, supported by NASA contract NSR-24-005-047 and administered by the University of Minnesota. I thank R. J. Collins and R. Smoluchowski for their encouragement.

10 January 1966

Low-Energy Protons: Average Flux in Interplanetary Space during the Last 100,000 Years

Abstract. *The radioactivity of aluminum-26 in two cores of Pacific sediments is an order of magnitude higher than was expected, as a result of its production by cosmic-ray interactions in the terrestrial environment. The higher activity can be explained only by postulating influx with extraterrestrial cosmic dust that had been exposed to significant flux of energetic particles capable of producing nuclear interactions. These particles may well be the "solar" cosmic rays that are sporadically accelerated by Sun during certain solar flares, since the steady galactic cosmic-ray flux is inadequate. The long-term average flux of low-energy protons in interplanetary space, required to yield the observed rate of influx of aluminum-26, is deduced on the basis of certain assumptions.*

Recent detection in our laboratory of Al^{26} in marine sediments (*1*) has implications regarding the long-term intensity of low-energy protons in interplanetary space. In this investigation several sections of two Pacific cores, up to 1 m in depth, were analyzed for activities of Al^{26} and Be^{10}. The radioactivity of Al^{26}, a positron emitter, was measured specifically by means of a sensitive gamma-gamma coincidence spectrometer; the observed signal in the 0.51-Mev photopeak was shown not to be due to the presence of contaminating activity. The summed coincidence spectra for all aluminum sam-

Table 1. Determinations of Be^{10} activity in samples from two cores of Pacific sediments; depths of water are in parentheses (*1*).

Core section		Density (dry wt:vol *in situ*)	Be^{10} conc. (dpm/kg, dry)
No.	Interval (cm)		
From 57°35'S, 174°15'W (4760 m)			
B	0–12	0.56	4.7 ± 0.5
C	12–27	.53	$4.6 \pm .4$
G	37.5–52.5	.51	$3.6 \pm .5$
H	52.5–67.5	.55	$3.0 \pm .5$
D	83–110	.45	$4.6 \pm .5$
From 8°20'N, 145°24'W (5110 m)			
E	0–21.5	0.39	$5.0 \pm .4$
A	100–120	.37	$2.1 \pm .4$

ples and background (taken with a Lucite disc of appropriate thickness) are shown in Fig. 1; relevant details of cores and results appear in Tables 1 and 2. The mean observed activities of Al^{26} for certain groupings of core samples are given in Table 2; we have not attempted to interpret the variation of Al^{26} activity with depth because of the large statistical errors due to its weak activity.

The mean ratio of activity, Al^{26}:Be^{10} (Table 2), in the two cores is 0.12 ± 0.04. The real ratio will be somewhat higher for two reasons. Firstly, the total Be^{10} activity of the core was extracted, whereas that of Al^{26} was measured mainly in the HCl-leach fraction only. Experiments showed that most of the Be^{10} activity appeared in the HCl-leach and therefore, by analogy, most of the Al^{26} activity was probably recovered. Secondly, the half-life of Al^{26} is 7.4×10^5 years, in contrast with 2.5×10^6 years for Be^{10}, and a small preferential decay of Al^{26} over Be^{10} is expected in lower sections of the sediment; this effect is probably small in magnitude, however, since the Be^{10} concentrations point to a sedimentation rate of about 4 mm/10^3 years (*1*).

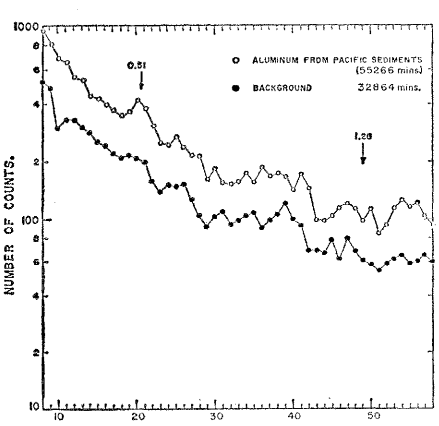

Fig. 1. Summed coincidence spectra of aluminum samples A, B, C, D, E, G, and H, extracted from marine sediments, and background. The detector is made of two sodium iodide crystals 6.4 cm in diameter and 3.8 cm thick. Channels 8 to 58 represent the energy interval 0.18 to 1.6 Mev.

The radionuclides Be^{10} and Al^{26} are expected to be produced on Earth mainly as results of spallations of atmospheric N and O and Ar nuclei, respectively (*2*); their global production rates have been estimated at 4.5×10^{-2} (Be^{10}) and 1.4×10^{-4} (Al^{26}) atom/cm^2 sec (*3*). Thus the expected $Al^{26} : Be^{10}$ ratio of activities in freshly deposited sediments is 0.01 (lower in older sediments), provided that terrestrial production alone was operative. The measured value, 0.12 ± 0.04, which is a lower limit to the activity ratio at deposition, is about an order of magnitude higher, and we shall now discuss its implications.

The geochemical behaviors of Be and Al in the oceans are expected to be identical; their mean time of residence in the ocean is short, so that one would not expect any enrichment of one relative to the other (*1, 4*). Furthermore, because Al^{26} is produced from nuclear disintegrations in Ar, which constitute only 0.9 percent of all atmospheric disintegrations (in N, O, and Ar), and because the yield of Al^{26} is clearly expected to be smaller in Ar disintegrations than that of Be^{10} in N and O, the calculations of Lal and Peters (*3*) can hardly be in error for the purpose of this discussion. Thus we must conclude that a mechanism must exist, for preferential production (and injection) of Al^{26}, in addition to that considered so far. If solar cosmic rays contributed significantly to isotope production in Earth's atmosphere (polar regions), such production would only lead to preferential production of Be^{10}, because the solar-cosmic-ray spectrum is richer in lower-energy particles and the threshold for production of Be^{10} is lower than that for Al^{26}. A wholly terrestrial production mechanism to explain the observed Al^{26}:Be^{10} ratio thus seems to be ruled out. It is also clear that any mechanism postulated to explain the observed ratio should produce Al^{26} more preferentially (over Be^{10}) than nuclear interactions of cosmic rays in the atmosphere.

The only other possible important mechanism seems to be the influx of meteorites and cosmic dust (micrometeorites), which will contain Al^{26} produced by interplanetary bombardment by cosmic-ray particles ("cosmic" being used in a very broad sense to include all particles energetic enough to produce nuclear reactions). In fact our search for Al^{26} was based on the idea (*4*) that its influx from extraterrestrial sources may be considerably greater than direct production in the atmosphere.

Fairly reliable estimates exist for the influx rates of meteorites (*5, 6*) and cosmic dust (*7*). The total mass influx of meteorites (primarily chondrites) to Earth is estimated at 1000 ton/year (*5, 6*). Even if one reckons that 90 percent of the original mass of the meteorite ablates in passage through the atmosphere, the fine ablated material thus strewn cannot amount to more than 50 tons of chondritic material per day on Earth. Assigning to this material the typical Be^{10} and Al^{26} concentrations found in typical-size chondrites (*8*), we have calculated upper limits for their average rates of influx.

The expected rate of influx of a radionuclide on Earth, $\bar{I}$, due to accretion of cosmic dust, is:

$$\bar{I} = M(P/\lambda)\ (1 - e^{-\lambda T}) \qquad (1)$$

where λ is the distintegration constant, T is the time of irradiation in space, P is the average rate of production of the radionuclide in the dust grains (averaged over time, T), and M is the rate of influx of cosmic dust. The value of P depends on the chemical composition of the dust, relevant excitation functions for formation of radionuclide in target nuclei of interest and importance (Si^{28}, Al^{27}, Mg^{26} for Al^{26}; O^{16} for Be^{10}), and the energy spectrum of cosmic-ray particles in space. Thus Eq. 1 shows that the rate of influx due to accretion of cosmic dust is a function of three parameters: mass and chemical composition of dust accreted, interplanetary flux and energy spectrum of cosmic-ray particles, and the time of irradiation in space before accretion by Earth.

For the case of a secular equilibrium (that is, $\lambda T >> 1$) and an influx rate of 10^4 tons of cosmic dust per day (*7*) (assuming the dust to have chondritic composition), we have separately calculated the expected Al^{26} and Be^{10} influx rates for the cases of (i) bombardment by the galactic cosmic-ray flux as observed at the top of Earth's atmosphere during a quiet solar period (*9*), and (ii) irradiation by a low-energy-rich beam as observed to be accelerated by Sun during certain solar flares. The solar-cosmic-ray spectrum is quite variable from event to event and even during an event; we have assumed a rigidity spectral shape that has been shown to hold good for several events over a wide range of energies (*10*). Three "typical" rigidity spectra are used for calculations (*11*), which are carried out in a manner similar to that adopted earlier (*12*, *13*). A simplifying assumption was made that solar cosmic rays are all protons.

The results for Al^{26} are summarized in Table 3, which includes the rate of total influx of Al^{26} required to explain the observed $Al^{26} : Be^{10}$ ratio in sediments; the influx rate is based on the estimated rate of global production of Be^{10}: 4.5×10^{-2} atom/cm²sec (*3*). We have considered here only the terrestrial production of Be^{10}, because it is found that its total influx from extraterrestrial sources under the conditions stipulated in rows 2 and 3 of Table 3 (which lead to a significant influx of Al^{26}) is less than 8×10^{-4} atom/cm² sec; thus the influx of extraterrestrial Be^{10} is expected to constitute no more than 2 per cent of its terrestrial production.

Table 2. Aluminum-26 concentrations and $Al^{26} : Be^{10}$ activity ratios in samples from two cores of Pacific sediments. Extraction of aluminum from sections A, B, and C and D, E, G, and H was about 50- and 82-percent chemically efficient, respectively; groupings could therefore be made only in limited ways.

Core sections		Al^{26} activity		
No.*	Interval (cm)	Count rate (cpm $\times 10^2$)†	Concentration (dpm/kg, dry)	To Be^{10} activity, ratio‡
B, C	0–27	$0.43 \pm .19$	$0.78 \pm .34$	$0.17 \pm .07$
D, G, H	37–110	$.23 \pm .14$	$.24 \pm .15$	$.07 \pm .04$
A, B, C	0–27, 100–120	$.29 \pm .15$	$.56 \pm .29$	$.15 \pm .08$
D, E, G, H	37–110, 0–21.5	$.30 \pm .13$	$.35 \pm .15$	$.09 \pm .04$

* See Table 1 for sources. † Mean net count rate in the 0.51-Mev coincidence channel. ‡ Estimated mean value, 0.12 ± 0.04.

Table 3. Global rates of terrestrial production and extraterrestrial influx of Al^{26}. The experimentally deduced total rate of influx is 1.6×10^{-3} atom/cm² sec; the two cores analyzed derived from latitudes 57 and 8°, and we assume that this rate corresponds to the global rate.

Al^{26}	
Source	Rate (atom/cm² sec)
Cosmic-ray spallation of atmospheric argon nuclei	1.4×10^{-4}
Ablation of typical-size chondritic meteorites (50 ton/day.Earth)	4×10^{-6}
Accretion of cosmic dust (10^4 ton/day.Earth) for the case of secular-equilibrium irradiation by:	
Galactic cosmic rays	7×10^{-5}
An omnidirectional flux of protons*	0.8×10^{-3} for $R_o = 50$
	1.2×10^{-3} for $R_o = 100$
	1.3×10^{-3} for $R_o = 150$

* Having the differential rigidity spectrum $dN = Ke^{-R/R_o}dR$, with $N > 10$ Mev = 20/cm² sec. The integrated flux above 10 Mev (R = 138 Mv) is kept fixed in the calculations. The threshold for A^{26} production is in the neighborhood of 10 Mev; therefore the production rate of Al^{26} per proton of kinetic energy higher than 10 Mev is nearly independent of R_o.

Table 3 shows that contribution from the ablation of meteorites falls short of the required influx of extraterrestrial Al^{26} (1.4×10^{-3} atom/cm² sec; difference between the deduced rate of total influx and the number in row 1) by a factor of 350 (*14*). The required influx of Al^{26} can be accounted for only by accretion of cosmic dust exposed to an omnidirectional flux of about 20 proton/cm² sec of $E > 10$ Mev, if a secular equilibrium is assumed. Considering the size distribution of cosmic dust (*7*) and the time scales involved in the heliocentric shrinkage of dust orbits, it seems that Al^{26} activity will, however, not reach secular equilibrium. It seems that for dust particles to spiral-in from 3 to 4 astronomical units (AU) the mean irradiation time T, of dust, is in the neighborhood of 10^5 years (*12*), corresponding to an undersaturation of Al^{26} activity by a factor of about 10. However, because there are other effects that may reduce the rate of orbit shrinkage, we shall assume a value of 5 for the mean undersaturation. This implies that the long-term average omnidirectional low-energy-proton flux (above 10 Mev) at about 2 AU has been about 100/cm² sec during the last (approximately) 10^5 years.

All discussion has been based so far on a chondritic composition of cosmic dust. The dust contributing to Al^{26} influx is expected to derive primarily from particles of from 10^{-10} to 10^{-6} g (*7*), for which an asteroidal, meteoric, or cometary origin is not yet determined. Thus, if particles in this mass range, sampled by satellite and rocket probes, are found to have higher content than chondrites, of elements lighter in mass than silicon, the true flux of low-energy protons will have to be correspondingly higher. Of the several available estimates of the rate of total influx of cosmic dust, the value adopted (10^4 ton/day.Earth) seems to be statistically and experimentally the best (*7*). However, if the mass influx of cosmic dust is somewhat less, as other considerations and observations in polar ice suggest (*6*, *12*), the low-energy-proton flux will have to be correspondingly higher.

Although there are now several uncertainties in the value 100/cm² sec that we have deduced for the flux of low-energy protons, $E > 10$ Mev, it seems to be a fairly conservative working value for consideration of its geophysical implications. It is hoped that the radiochemical data themselves may provide answers for these parameters. The two other activities, of Mn^{53} and Ni^{59}, that are similarly expected to be accreted by Earth, should be detectable (*4*, *11*). Clues to the chemical composition of cosmic dust may come from measurements of the influx of Mn^{53} that will be produced by interactions in iron nuclei. On the other hand, comparison of the activities of Al^{26} and Mn^{53} with that of Ni^{59}, whose half-life is as short as 8×10^4 years, may provide an entry into the problem of rate of heliocentric shrinkage. Detailed calculations of the expected rates of influx of these nuclides, and the problem of their detection, will be discussed elsewhere (*11*).

Finally we may mention that on the basis of observations of solar-cosmic-ray events Webber (*15*) has deduced that the flux of solar protons of more than 10 Mev was 150/cm² sec during 1954–63, and that during a typical solar cycle the corresponding flux would be about 30/cm² sec. It is gratifying to see the general agreement between the present radiochemical value and that based on observations of solar-cosmic-ray events, which, however, besides being limited in number are confined essentially to one solar cycle.

D. LAL*
V. S. VENKATAVARADAN
Tata Institute of Fundamental Research, Colaba, Bombay 5, India

References and Notes

1. B. S. Amin, D. P. Kharkar, D. Lal, *Deep-Sea Research*, in press.
2. Production of these nuclides in the surface crustal materials by nuclear interactions, and their subsequent introduction to the oceans, constitutes a minor source (see *1*, *12*).
3. D. Lal and B. Peters, *Handbuch der Physik* (Springer, Berlin, in press), vol. 2, *Cosmic Rays*.
4. D. Lal, *J. Oceanog. Soc. Japan 20th Anniv. Vol.* (1962), p. 600; *Earth Science and Meteoritics* (North-Holland, Amsterdam, 1963), p. 115.
5. E. Anders, *Space Sci. Rev.* **3**, 583 (1964).
6. P. W. Hodge, F. W. Wright, C. C. Langway, Jr., *J. Geophys. Res.* **69**, 2919 (1964).
7. W. M. Alexander, C. W. McCraken, L. Secretan, O. E. Berg, *Space Research III* (North-Holland, Amsterdam, 1963), p. 891.
8. M. Honda, S. Umemoto, J. R. Arnold, *J. Geophys. Res.* **66**, 3541 (1961).
9. F. B. McDonald and W. R. Webber, *Phys. Rev.* **115**, 194 (1959).
10. P. S. Freier and W. R. Webber, *J. Geophys. Res.* **68**, 1605 (1963).
11. D. Lal and V. S. Venkatavaradan, in preparation.
12. J. T. Wasson, *Icarus*, **2**, 54 (1963).
13. J. R. Arnold, M. Honda, D. Lal, *J. Geophys. Res.* **66**, 3519 (1961).
14. This conclusion is not modified even if we consider that the albation material may have an Al^{26} activity higher than that observed in chondrites sampled, because of production of Al^{26} in its outermost layers by solar cosmic rays.
15. W. R. Webber, private communication.

16. We thank G. Arrhenius for providing the sediment cores and J. R. Arnold and R. R. Daniel for stimulating and helpful discussions.

* Present address: Institute of Geophysics and Planetary Physics, University of California, Los Angeles 90024.

1 November 1965

Rotation of Mercury: Theoretical Analysis of the Dynamics of a Rigid Ellipsoidal Planet

Abstract. *The second-order nonlinear differential equation for the rotation of Mercury implies locked-in motion when the period is within the range*

$$\frac{2T}{3}\left[1-\lambda\cos\frac{2\pi t}{T} \pm \frac{2}{3}(21\lambda e/2)^{\frac{1}{2}}\right]$$

where e *is the eccentricity and* T *is the period of Mercury's orbit, the time* t *is measured from perihelion, and* λ *is a measure of the planet's distortion. For values near* 2T/3, *the instantaneous period oscillates about* 2T/3 *with period* $(21\lambda e/2)^{-\frac{1}{2}}T$.

Radar (*1*) and visual (*2*) observations of the planet Mercury indicate a rotation period $T_r = 58.4 \pm 0.4$ days, close to ⅔ of the orbit period $T = 87.97$ days. Colombo (*3*) and Liu and O'Keefe (*4*) have surmised that a stable "locked-in" motion of this type can occur as a result of the inverse-cube term in the planetary potential (*5, 6*) that arises for a body with unequal moments of inertia in the orbital plane. The existence of such a solution to the equations that govern the rotation of a rigid distorted planet has been demonstrated by Liu and O'Keefe by means of digital computations. In this report we present approximate analytic formulas that may afford further physical insight into the character of locked-in motion, that could facilitate the interpretation of observational data, and that indicate the dependence of the results upon the various parameters of the model. For simplicity, and for clarity in exposition, the analysis is carried to no higher order than is required to exhibit the salient features of the phenomenon.

The differential equation for the orientation, θ, of the planet is given by equation 4 of the report by Liu and O'Keefe (*4*). In terms of the variable $\tau = 2\pi t/T$ it becomes, after insertion of the equation for the Keplerian orbit (*7*) of eccentricity e,

$$\frac{d^2\theta}{d\tau^2}+\frac{3}{2}\lambda\left[\frac{1+e\cos f(\tau)}{1-e^2}\right]^3\times \sin 2[\theta - f(\tau)] = 0 \qquad (1)$$

with the largest of the principal moments of inertia (C) taken perpendicular to the orbital plane, $\lambda \equiv (B-A)/C$ measuring the difference between the two smaller moments of inertia (B and A), and f denoting the true anomaly. (Since damping effects have been ignored in this analysis, Eq. 1 is derivable from a simple Hamiltonian function, with periodic coefficients, in which $p = d\theta/d\tau$ is the canonical momentum conjugate to θ, and Liouville's theorem concerning the conservation of phase-space area applies to the variables θ and p.)

Substitution of the explicit variation of the true anomaly with time, as given by

$$f(\tau) = \tau + 2e\sin\tau \qquad (2)$$

through the first-order term in e, converts Eq. 1 to the approximate form

$$\frac{d^2\theta}{d\tau^2}+\frac{3}{2}\lambda\Big[(1+3e\cos\tau)\sin 2(\theta-\tau) - 4e\sin\tau\cos 2(\theta-\tau)\Big] = 0 \qquad (3)$$

which forms the basis of the remainder of our analysis. [It is noted, from Eq. 2, that τ is to be regarded as measured from the time of perihelion passage, and θ is the angle made by the smallest of the moments of inertia (A) with the major axis of the orbit.] One expects that there may be periodic (locked-in) solutions to Eqs. 1 or 3 that are stable, in the sense that neighboring solutions describe oscillatory motion about these periodic solutions.

We consider, specifically, solutions for which

$$d\theta/dt \approx (3/2)(2\pi/T)$$

and write

$$\theta = \frac{3}{2}\tau + \eta, \qquad (4)$$

so that Eq. 3 becomes

$$\frac{d^2\eta}{d\tau^2}+\frac{3}{2}\lambda\Big[(\cos\tau+\frac{7}{2}e - \frac{1}{2}e\cos 2\tau)\sin 2\eta + (\sin\tau - \frac{1}{2}e\sin 2\tau)\cos 2\eta\Big] = 0 \qquad (5)$$

When η is small, Eq. 5 may be linearized, to assume the form

$$\frac{d^2\eta}{d\tau^2}+\frac{3}{2}\lambda\,(2\cos\tau + 7e - e\cos 2\tau)\eta = -\frac{3}{2}\lambda(\sin\tau - \frac{1}{2}e\sin 2\tau) \qquad (6)$$

For $\lambda^2 \ll 1$, an approximate particular integral to the inhomogeneous Eq. 6 is readily obtained, and the solution to the corresponding linear homogeneous equation may be derived (*8*) by ignoring terms of average value zero in the coefficient of η. The solution thus includes a periodic motion, of period T, and a long-period oscillation of amplitude α_0:

$$\eta = \frac{3}{2}\lambda(\sin\tau - \frac{1}{8}e\sin 2\tau) + \alpha_0\sin\left[(\frac{21}{2}\lambda e)^{\frac{1}{2}}\tau + \alpha_1\right] \qquad (7a)$$

or, for $\alpha_0 \ll \pi$,

$$\theta = \frac{3\pi t}{T} + \frac{3}{2}\lambda(\sin\frac{2\pi t}{T} - \frac{1}{8}e\sin\frac{4\pi t}{T}) + \alpha_0\sin\left[(\frac{21}{2}\lambda e)^{\frac{1}{2}}\frac{2\pi t}{T} + \alpha_1\right] \qquad (7b)$$

where α_0 and α_1 are arbitrary constants.

If α_0 is not small, so that the slow excursions of η preclude linearization, a similar averaging of the coefficient of $\sin 2\eta$ in Eq. 5 suggests that these oscillations are essentially described by an equation of the form applicable to the motion of a physical pendulum:

$$\frac{d^2\eta}{d\tau^2} + \frac{21}{4}\lambda e\sin 2\eta = 0 \qquad (8)$$

for which one may write the first integral

$$\frac{1}{2}(\frac{d\eta}{dt})^2 - \frac{21}{8}\lambda e\cos 2\eta = c \qquad (9)$$

where c is a constant. With the excursions of η limited to $\pm\pi/2$ for oscillatory motion, the *maximum* value that